Draft version August 12, 2019
Typeset using LaTeX **modern** style in AASTeX62

A Two Percent Measurement

Will M. Farr,[1,2] Maya Fishbach,[3] Jiani Ye,[1] and Daniel E. Holz[4]

[1] *Department of Physics and Astronomy, Stony Brook University, Stony Brook NY 11794, USA*
[2] *Center for Computational Astronomy, Flatiron Institute, 162 5th Ave., New York NY 10010, USA*
[3] *Department of Astronomy and Astrophysics, University of Chicago, Chicago IL 60637, USA*
[4] *Enrico Fermi Institute, Department of Physics, Department of Astronomy and Astrophysics, and Kavli Institute for Cosmological Physics, University of Chicago, Chicago IL 60637, USA*

ABSTRACT

Simultaneous measurements of distance and redshift can be used to constrain the expansion history of the universe and associated cosmological parameters CITE. Merging binary black hole (BBH) systems are standard sirens (Schutz 1986; Holz & Hughes 2005)—their gravitational waveform provides direct information about the luminosity distance to the source. Because gravity is scale-free, there is a perfect degeneracy between the source masses and redshift; some non-gravitational information is necessary to break the degeneracy and determine the redshift of the source (Schutz 1986; Chernoff & Finn 1993; Finn 1996; Wang & Turner 1997; Holz & Hughes 2005; Dalal et al. 2006; Taylor et al. 2012; Messenger & Read 2012; Abbott et al. 2017; Fishbach et al. 2019; Soares-Santos et al. 2019). Here we suggest that the pair instability supernova (PISN) (Heger & Woosley 2002; Belczynski et al. 2016; Woosley 2017; Spera & Mapelli 2017) process, thought to be the source of the observed upper-limit on the black hole (BH) mass in merging BBH systems at $\sim 45\,M_\odot$ (The LIGO Scientific Collaboration et al. 2018a), imprints a mass scale in the population of BBH mergers and permits a measurement of the redshift-luminosity-distance relation with these sources. We simulate five years of BBH detections in the Advanced LIGO and Virgo detectiors with realistic assumptions about the BBH merger rate (The LIGO Scientific Collaboration et al. 2018b), a mass distribution incorporating a PISN mass scale (The LIGO Scientific Collaboration et al. 2018a), and measurement uncertainty (Vitale et al. 2017). We show that after one year of operation at design sensitivity (put date here) the BBH population can constrain $H(z)$ to 6.1% at a pivot redshift $z \simeq 0.8$.

will.farr@stonybrook.edu
mfishbach@uchicago.edu
jiani.ye@stonybrook.edu
holz@uchicago.edu

After five years (date) the constraint improves to 2.9%. This measurement relies only on general relativity and the presence of a cutoff mass scale that is approximately fixed or calibrated across cosmic time ($\partial M_{\rm scale}/\partial z \lesssim 1\,M_\odot$); it is independent of any distance ladder or cosmological model. When combined with a percent-level local measurement of the Hubble constant (Chen et al. 2017) and a sub-percent constraint on the physical matter density from CMB measurements (Planck Collaboration et al. 2016) in a wCDM cosmological model, the dark energy equation of state parameter is determined with 12% uncertainty. Observations by future "third-generation" gravitational wave (GW) detectors CITE, which can see BBH mergers throughout the universe, would permit sub-percent cosmographical measurements to $z \gtrsim 4$ within one month of observation.

The gravitational wave transient catalog 1 (GWTC1) contains ten binary black hole merger events observed during Advanced LIGO and Advanced VIRGO's first and second observing runs (The LIGO Scientific Collaboration et al. 2018b). Modeling of this population suggests a precipitous drop in the merger rate for primary black hole masses larger than $\sim 45\,M_\odot$ (Fishbach & Holz 2017; The LIGO Scientific Collaboration et al. 2018b). A possible explanation for this drop is the PISN process CITE. This process occurs in the cores of massive stars (helium core masses 30–133 $M_\odot$ (Woosley 2017)) when the core temperature becomes sufficiently high to permit the production of electron-positron pairs; pair production softens the equation of state of the core, leading to a collapse which is halted by nuclear burning (Heger & Woosley 2002). The energy produced can either unbind the star, leaving no BH remnant, or drive a mass-loss pulse that reduces the mass of the star until the PISN is halted, leading to remnant masses $\sim 45\,M_\odot$. Modeling suggests that the upper limit on the remnant mass may vary by less than XX with redshift for $0 \leq z \lesssim 2$ (Belczynski et al. 2016).

Compact object mergers that emit gravitational waves have a universal characteristic peak luminosity $c^5/G \simeq 3.6 \times 10^{59}\,{\rm erg\,s^{-1}}$ that enables direct measurements of the luminosity distance to these sources (Schutz 1986). They are standard sirens (Holz & Hughes 2005). However, the effects of the source-frame mass and redshift are degenerate in the gravitational waveform; the observed waveform depends only on the redshifted mass in the detector frame, $m_{\rm det} = m_{\rm source}(1+z)$. General relativity predicts the gravitational waveforms of stellar-mass BBH mergers. Using parameterized models of these waveforms (Taracchini et al. 2014; Khan et al. 2016; Bohé et al. 2017; Chatziioannou et al. 2017), it will be possible to measure the detector-frame masses with $\sim 20\%$ uncertainty and luminosity distances (Hogg 1999) with $\sim 50\%$ uncertainty for a source near the detection threshold in Advanced LIGO and Anvanced Virgo at design sensitivity (Vitale et al. 2017). The uncertainty in these parameters scales inversely with the signal-to-noise ratio of a source.

If the BBH merger rate follows the star formation rate (Fishbach et al. 2018; The LIGO Scientific Collaboration et al. 2018a), the primary mass distribution follows a declining power law $m_1^{-\alpha}$ with $\alpha \simeq 0.75$ for $m_1 \lesssim 45\,M_\odot$, tapering off above this mass scale, the mass ratio distribution is flat, and the three-detector duty cycle is $\sim 50\%$ then Advanced LIGO and Advanced Virgo should detect ~ 1000 BBH mergers per year at design sensitivity over a range of redshifts $0 \leq z \lesssim 1.5$. The typical detected merger will have a redshift $z \sim 0.5$. If we assume that $\sim 1/4$ these detections are informative about the redshifted upper limit on the remnant mass in the detector frame, $m_{\rm max,det} = m_{\rm max,source}\,(1 + z\,(d_L))$, that the combined uncertainty is $1/\sqrt{N}$ smaller than the single-measurement uncertainty, and that most detections are near threshold, then we are dominated by the $\sim 50\%$ distance uncertainty and can achieve an absolute distance-redshift measurement (i.e. constrain the local expansion rate, $H(z)$, for $z \simeq 0.75$) at the $50\%/\sqrt{1000/4} \simeq 3\%$ level after one year, and the 1.4% level after five years of BBH merger observations at design sensitivity.

Detailed calculations are within a factor of two of this back-of-the-envelope estimate. We have simulated five years of GW observations with Advanced LIGO and Advanced Virgo at design sensitivity. We use a local merger rate, mass distribution, and rate evolution with redshift that are consistent with current observations (Fishbach & Holz 2017; Fishbach et al. 2018; The LIGO Scientific Collaboration et al. 2018a). Our mass distribution tapers off at $m = 45\,M_\odot$ to model the effects of the PISN process (Belczynski et al. 2016). We use a realistic model of the detectability of sources from this population (Abbott et al. 2016a,b) and for mass and distance estimation uncertainties (Vitale et al. 2017). The properties of the simulated population are described more fully in §A. Figure 1 shows the simulated detections and uncertainty for one and five years of observation.

We fit a parameterized model of the true mass distribution to this data set accounting for measurement error and selection effects in a hierarchical analysis (Hogg et al. 2010; Mandel 2010; Loredo 2004; Mandel et al. 2019; Farr 2019). We include parameters for the power-law slopes in the mass distribution and redshift evolution, a mass scale and range of masses over which the mass distribution cuts off due to the PISN, a parameterized FLRW cosmology with H_0, Ω_M, and w free parameters (Hogg 1999), and parameters for the true masses and redshift of each detected signal. The "population-level" distribution and cosmological parameters are given broad priors that are much wider than the corresponding posteriors. Marginalizing over all parameters except H_0, Ω_M and w induces a posterior over expansion histories, $H(z)$, that is shown in Figure 2. The redshift at which the fractional uncertainty in $H(z)$ is minimized—the "pivot" redshift—is 0.8. After one year of observations, the fractional uncertainty in $H(z = 0.8)$ is 6.1%; after five years it is 2.9%. This demonstrates an absolute distance measure to $z \simeq 0.8$ at percent-level precision; combining this inference on $H(z)$ with other data sets such as observations of baryon acoustic oscillations (Aubourg et al. 2015) or Type Ia supernovae (Scolnic et al. 2018) can translate this

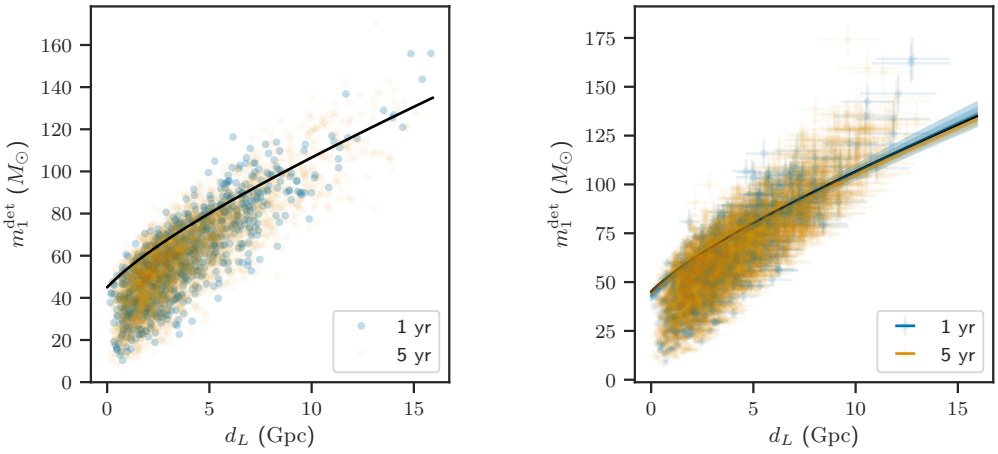

Figure 1. Simulated population of BBH mergers. (Left) The true detector-frame primary BH masses and luminosity distances for the simulated population of BBH mergers used in this work. Blue circles denote one year of Advanced LIGO / Virgo observations, orange circles five years of observations. The black line shows the redshifting of the PISN BH mass scale corresponding to the cosmology used to generate the events (Planck Collaboration et al. 2016, TT, TE, EE + lowP + lensing + ext). (Right) The inferred detector-frame primary BH masses and luminosity distances using our model of the measurement uncertainty for each event. Here again blue corresponds to one year of observations and orange to five years. Dots denote the mean and bars the 1σ width of the likelihood for each event. There is a bias in the recovery of the masses and distance that becomes more acute at large distances due to a failure to model the population (which is not flat in m_1 and d_L) and selection effects in these single-event analyses. The black line shows the redshifting of the PISN mass scale. The most-distant event biases upward in both mass and distance by several sigma because it represents a single "lucky" noise fluctuation into detectability out of $\sim 2 \times 10^5$ merger events per year within the detector horizon. We also show the inferred distance-mass relation from our analysis of the one year and five year mock data sets in the same colors (the solid line gives the posterior median, dark band gives the 68% credible interval, and the light band the 95% credible interval).

absolute distance measure to other redshifts (at $z = 0$ it would correspond to an uncertainty on H_0 of $\pm 2.0\,\mathrm{km\,s^{-1}\,Mpc^{-1}}$) (Aubourg et al. 2015; Cuesta et al. 2015; Feeney et al. 2019). For example, one can independently calibrate the Type Ia supernova distance scale without a distance ladder (Feeney et al. 2019; Scolnic et al. 2018), or compare the GW-determined distance scale with one derived from the photon-baryon sound horizon (Cuesta et al. 2015; Aylor et al. 2019) in the early universe (Planck Collaboration et al. 2016) or at late times (Aubourg et al. 2015).

Our hierarchical model also estimates the source-frame masses and redshifts for each individual event that incorporate our information about the population. These results for the one-year data set are shown in Figure 3. Events pile up near the PISN mass scale; in effect, the cosmology is adjusted so that the measured distances to each event generate redshifts that produce a constant PISN mass scale in the source-frame from measured detector-frame masses.

The pivot redshift for this measurement is close to the redshift where the physical matter and dark energy densities are equal, and thus this measurement can be in-

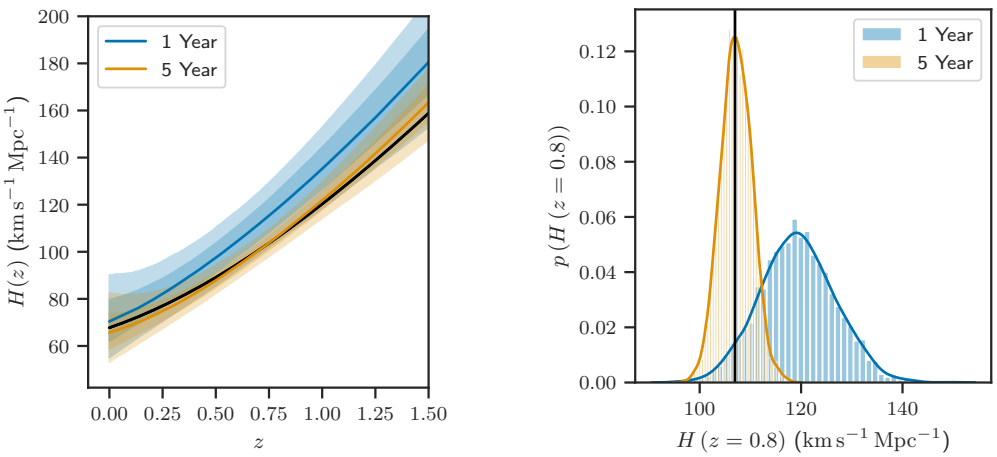

Figure 2. Inferred cosmological expansion history and distance scale. (Left) The local expansion rate, $H(z)$, inferred from an analysis of the one year (blue) and five year (orange) simulated populations using a mass distribution model with a parameterized cutoff mass (see text). The black line gives the cosmology used to generate the simulated population (Planck Collaboration et al. 2016, TT, TE, EE + lowP + lensing + ext). The solid lines give the posterior median $H(z)$ at each redshift; the bands give 1σ (68%) and 2σ (95%) credible intervals. The 1σ fractional uncertainty on $H(z)$ is minimized at $z \simeq 0.8$ for both data sets; after one year it is 6.1 % and after five years it is 2.9 %. (Right) Posterior distributions over $H\,(z = 0.8)$, corresponding to the redshift where the fractional uncertainty is minimized. The true $H\,(z = 0.8)$ is shown by the black vertical line. The posterior after one year is blue, after five years is orange.

formative about the dark energy equation of state. If we assume an independent 1% measurement of H_0 (as could be obtained from GW observations of binary neutron star (BNS) mergers with identified electromagnetic counterparts (Chen et al. 2017)) and a measurement of the physical matter density at high redshift (as obtained by the Planck satellite's measurements of the cosmic microwave background (CMB) (Planck Collaboration et al. 2016)), then the remaining un-constrained parameter in our cosmological model is w, the dark energy equation of state. Imposing these additional measurements as a tight prior on the relevant parameters, we find that our synthetic population of BBH mergers can constrain w to 19% and 12% after one and five years of observations. These measurements would be competitive with, but independent from, other constraints on w CITE. Posteriors for w with these informative priors are shown in Figure 4.

Our simplistic analysis here assumes that the mass distribution of merging BBHs does not change with redshift. In reality the mass distribution will change because the metallicity of BBH progenitor systems changes with redshift CITE. The PISN mass scale, however, is not expected to evolve much to $z \simeq 1.5$ CITE. Is it? This one is for Daniel. We infer a mass scale in our simple model of $44.64^{+0.76}_{-0.81}\,M_\odot$ after five years; changes in the PISN mass scale for merging BBH systems at a comparable level to $z \simeq 5$ are a systematic that must be calibrated to ensure an accurate measurement. BBH mergers thus become "standardizable sirens" CITE.

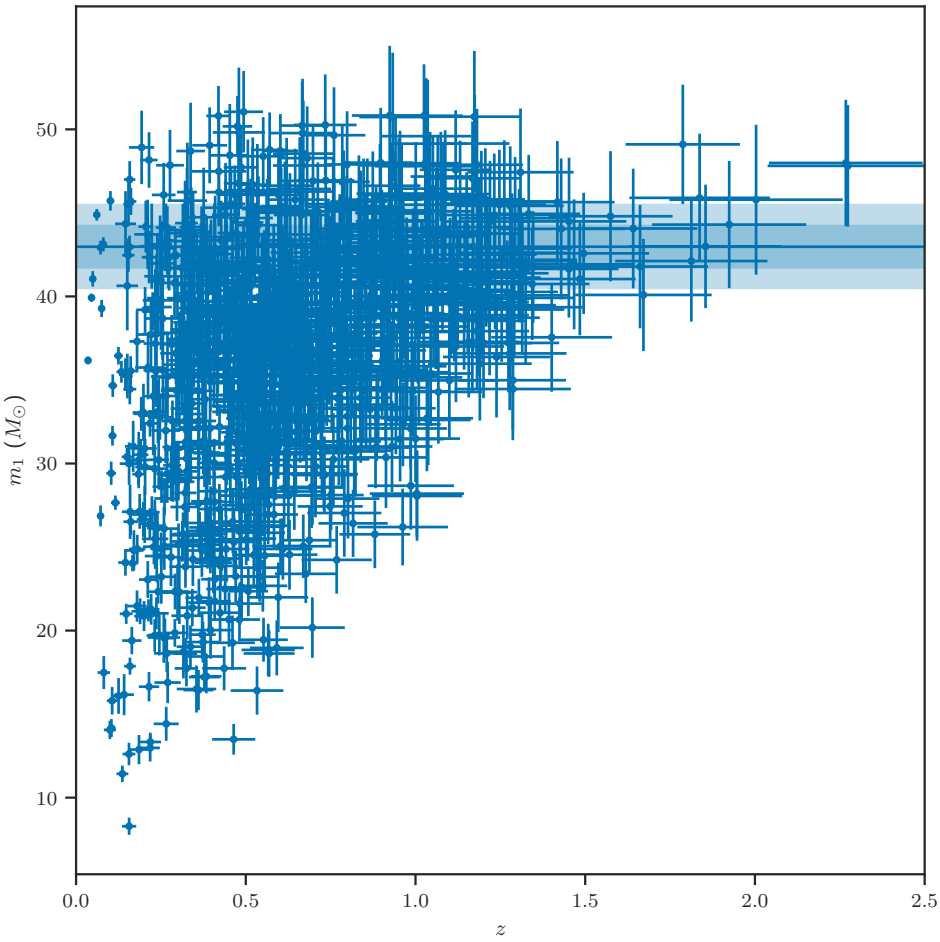

Figure 3. Inferred maximum mass and masses and redshifts for one year of observation. Posterior mean and 1σ (68%) credible ranges for the source-frame primary BH mass and redshift after one year of BBH merger observations. The horizontal line is the posterior median of the maximum black hole mass set by the PISN process; the dark and light bands correspond to the 1σ and 2σ (68% and 95%) credible intervals on the maximum mass. (Compare to Figure 1.) Our model adjusts cosmological parameters, and therefore the correspondence between the measured detector-frame masses and luminosity distances and inferred redshifts and source-frame masses, until it achieves a consistent upper limit on the source-frame BH mass across all redshifts. After one year of synthetic observations we measure $M_{\rm scale} = 43.0^{+1.3}_{-1.3}\,M_\odot$ (median and 68% credible interval). After five years (not shown) we measure $M_{\rm scale} = 44.64^{+0.76}_{-0.81}\,M_\odot$.

Third generation GW detectors, planned for construction in the mid-2030s, would detect $\sim 15,000$ BBH mergers per month to $z \gtrsim 10$, with a typical relative uncertainty on d_L of $\sim 10\%$ at $z \simeq 2$ (Vitale & Farr 2018). Provided the PISN mass scale is properly calibrated, such detectors could achieve sub-percent uncertainty in cosmography to high redshifts $z \lesssim 5$ within *one month* of BBH merger observations.

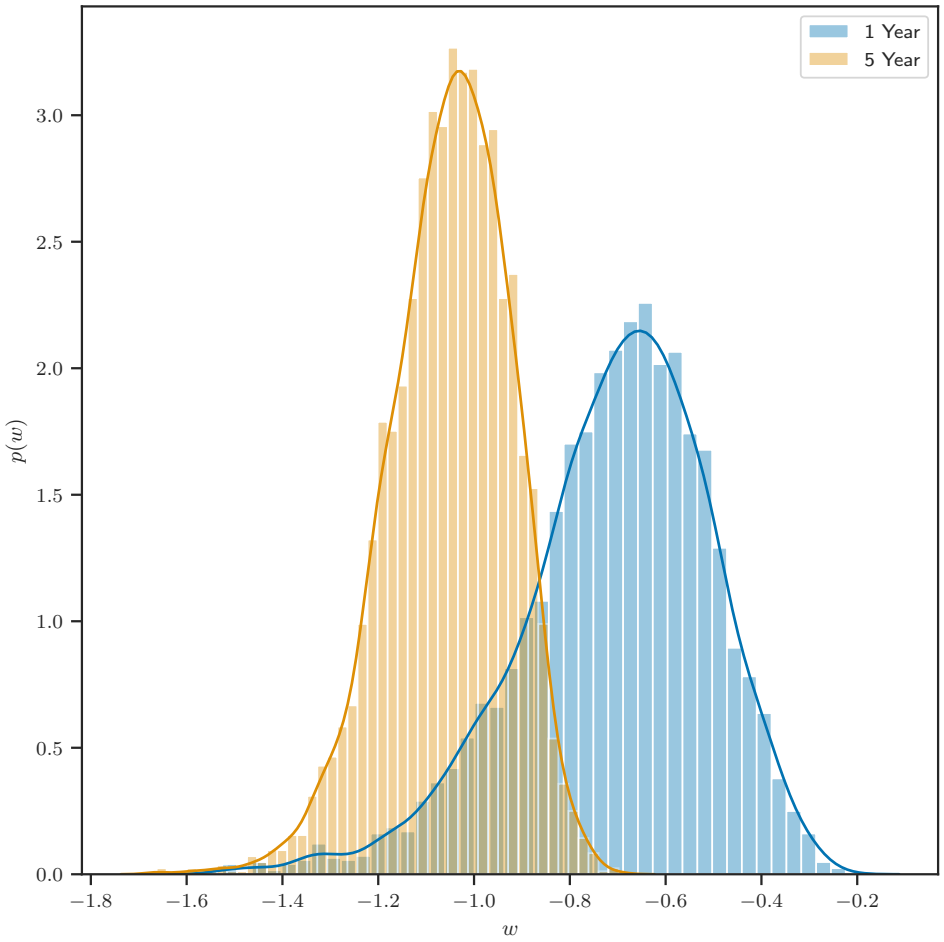

Figure 4. Posterior on the dark energy equation of state parameter after imposing additional cosmological constraints. If we impose a 1% measurement of H_0 (Chen et al. 2017; Mortlock et al. 2018) and the constraints on $\Omega_M h^2$ from existing observations of the cosmic microwave background (Planck Collaboration et al. 2016), we can infer the equation of state parameter $w_{\rm DE} \equiv P_{\rm DE}/\rho_{\rm DE}$ for dark energy in a wCDM cosmological model. (We do not obtain any meaningful constraint on the evolution of $w_{\rm DE}$ with redshift when this parameter is allowed to vary, so we fix it to a constant across all redshifts.) We use $w_{\rm DE} = -1$ to generate our data set; this value is indicated by the black line above. The posterior obtained on $w_{\rm DE}$ after one year of synthetic observations is shown in blue and after five years in orange. We find $w_{\rm DE} = -0.68^{+0.17}_{0.21}$ after one year (median and 68% credible interval) and $w_{\rm DE} = -1.04^{+0.12}_{0.13}$ after five years.

We thank Stephen Feeney for providing a sounding board for the methods discussed in this paper. We acknowledge the 2018 April APS Meeting and Barley's Brewing Company in Columbus, OH, USA where this work was originally conceived.

REFERENCES

Abbott, B. P., Abbott, R., Abbott, T. D., et al. 2016a, ApJ, 833, L1, doi: 10.3847/2041-8205/833/1/L1

—. 2016b, The Astrophysical Journal Supplement Series, 227, 14, doi: 10.3847/0067-0049/227/2/14

—. 2017, Nature, 551, 85, doi: 10.1038/nature24471
Aubourg, É., Bailey, S., Bautista, J. E., et al. 2015, PhRvD, 92, 123516, doi: 10.1103/PhysRevD.92.123516
Aylor, K., Joy, M., Knox, L., et al. 2019, ApJ, 874, 4, doi: 10.3847/1538-4357/ab0898
Belczynski, K., Heger, A., Gladysz, W., et al. 2016, A&A, 594, A97, doi: 10.1051/0004-6361/201628980
Bohé, A., Shao, L., Taracchini, A., et al. 2017, PhRvD, 95, 044028, doi: 10.1103/PhysRevD.95.044028
Chatziioannou, K., Klein, A., Yunes, N., & Cornish, N. 2017, PhRvD, 95, 104004, doi: 10.1103/PhysRevD.95.104004
Chen, H.-Y., Fishbach, M., & Holz, D. E. 2017, ArXiv e-prints, arXiv:1712.06531. https://arxiv.org/abs/1712.06531
Chernoff, D. F., & Finn, L. S. 1993, ApJ, 411, L5, doi: 10.1086/186898
Cuesta, A. J., Verde, L., Riess, A., & Jimenez, R. 2015, MNRAS, 448, 3463, doi: 10.1093/mnras/stv261
Dalal, N., Holz, D. E., Hughes, S. A., & Jain, B. 2006, PhRvD, 74, 063006, doi: 10.1103/PhysRevD.74.063006
Farr, W. M. 2019, Research Notes of the American Astronomical Society, 3, 66, doi: 10.3847/2515-5172/ab1d5f
Feeney, S. M., Peiris, H. V., Williamson, A. R., et al. 2019, PhRvL, 122, 061105, doi: 10.1103/PhysRevLett.122.061105
Finn, L. S. 1996, PhRvD, 53, 2878, doi: 10.1103/PhysRevD.53.2878
Fishbach, M., & Holz, D. E. 2017, ApJ, 851, L25, doi: 10.3847/2041-8213/aa9bf6
Fishbach, M., Holz, D. E., & Farr, W. M. 2018, ArXiv e-prints, arXiv:1805.10270. https://arxiv.org/abs/1805.10270
Fishbach, M., Gray, R., Magaña Hernandez, I., et al. 2019, ApJL, 871, L13, doi: 10.3847/2041-8213/aaf96e
Heger, A., & Woosley, S. E. 2002, ApJ, 567, 532, doi: 10.1086/338487
Hogg, D. W. 1999, ArXiv e-prints, astro. https://arxiv.org/abs/astro-ph/9905116
Hogg, D. W., Myers, A. D., & Bovy, J. 2010, ApJ, 725, 2166, doi: 10.1088/0004-637X/725/2/2166
Holz, D. E., & Hughes, S. A. 2005, ApJ, 629, 15, doi: 10.1086/431341
Khan, S., Husa, S., Hannam, M., et al. 2016, PhRvD, 93, 044007, doi: 10.1103/PhysRevD.93.044007
Loredo, T. J. 2004, in American Institute of Physics Conference Series, Vol. 735, American Institute of Physics Conference Series, ed. R. Fischer, R. Preuss, & U. V. Toussaint, 195–206
Mandel, I. 2010, PhRvD, 81, 084029, doi: 10.1103/PhysRevD.81.084029
Mandel, I., Farr, W. M., & Gair, J. R. 2019, MNRAS, 486, 1086, doi: 10.1093/mnras/stz896
Messenger, C., & Read, J. 2012, PhRvL, 108, 091101, doi: 10.1103/PhysRevLett.108.091101
Mortlock, D. J., Feeney, S. M., Peiris, H. V., Williamson, A. R., & Nissanke, S. M. 2018, arXiv e-prints, arXiv:1811.11723. https://arxiv.org/abs/1811.11723
Planck Collaboration, Ade, P. A. R., Aghanim, N., et al. 2016, A&A, 594, A13, doi: 10.1051/0004-6361/201525830
Schutz, B. F. 1986, Nature, 323, 310, doi: 10.1038/323310a0
Scolnic, D. M., Jones, D. O., Rest, A., et al. 2018, ApJ, 859, 101, doi: 10.3847/1538-4357/aab9bb
Soares-Santos, M., Palmese, A., Hartley, W., et al. 2019, ApJL, 876, L7, doi: 10.3847/2041-8213/ab14f1
Spera, M., & Mapelli, M. 2017, MNRAS, 470, 4739, doi: 10.1093/mnras/stx1576
Taracchini, A., Buonanno, A., Pan, Y., et al. 2014, PhRvD, 89, 061502, doi: 10.1103/PhysRevD.89.061502
Taylor, S. R., Gair, J. R., & Mandel, I. 2012, PhRvD, 85, 023535, doi: 10.1103/PhysRevD.85.023535

The LIGO Scientific Collaboration, the Virgo Collaboration, Abbott, B. P., et al. 2018a, arXiv e-prints, arXiv:1811.12940. https://arxiv.org/abs/1811.12940

—. 2018b, arXiv e-prints, arXiv:1811.12907. https://arxiv.org/abs/1811.12907

Vitale, S., & Farr, W. M. 2018, arXiv e-prints, arXiv:1808.00901. https://arxiv.org/abs/1808.00901

Vitale, S., Lynch, R., Raymond, V., et al. 2017, PhRvD, 95, 064053, doi: 10.1103/PhysRevD.95.064053

Wang, Y., & Turner, E. L. 1997, PhRvD, 56, 724, doi: 10.1103/PhysRevD.56.724

Woosley, S. E. 2017, ApJ, 836, 244, doi: 10.3847/1538-4357/836/2/244

APPENDIX

A. SIMULATED POPULATION

We draw our synthetic observations from a population that follows

$$\frac{\mathrm{d}N}{\mathrm{d}m_1\mathrm{d}m_2\mathrm{d}V\,\mathrm{d}t} = \frac{R_{30}}{(30\,M_\odot)^2}\left(\frac{m_1}{30\,M_\odot}\right)^{-\alpha}\left(\frac{m_2}{30\,M_\odot}\right)^{\beta}(1+z)^{\gamma} \times f_{\mathrm{smooth}}\left(m_1 \mid m_l, \sigma_l, m_h, \sigma_h\right) f_{\mathrm{smooth}}\left(m_2 \mid m_l, \sigma_l, m_h, \sigma_h\right), \quad \text{(A1)}$$

where all quantities are evaluated in the comoving frame and

$$f_{\mathrm{smooth}}\left(m \mid m_l, \sigma_l, m_h, \sigma_h\right) = \Phi\left(\frac{\log m - \log m_l}{\sigma_l}\right)\left[1 - \Phi\left(\frac{\log m - \log m_h}{\sigma_h}\right)\right] \quad \text{(A2)}$$

is a function that tapers smoothly to zero when $m \lesssim m_l$ or $m \gtrsim m_h$ over a scale in log-mass of σ_l and σ_h; $\Phi(x)$ is the standard normal cumulative distribution function. (We enforce $m_2 \leq m_1$.)

We have chosen population parameters that are consistent with the current observations reported in GWTC-1 (The LIGO Scientific Collaboration et al. 2018b,a):

$$R_{30} = 64.4 \quad \text{(A3)}$$
$$\alpha = 0.75 \quad \text{(A4)}$$
$$\beta = 0.0 \quad \text{(A5)}$$
$$\gamma = 3.0 \quad \text{(A6)}$$
$$m_l = 5\,M_\odot \quad \text{(A7)}$$
$$m_h = 45\,M_\odot \quad \text{(A8)}$$
$$\sigma_l = 0.1 \quad \text{(A9)}$$
$$\sigma_h = 0.1. \quad \text{(A10)}$$

with these choices the volumetric merger rate at $z = 0$ is $60\,\mathrm{Gpc}^{-3}\,\mathrm{yr}^{-1}$. The corresponding marginal mass distributions for m_1 and m_2 are shown in Figure 1.

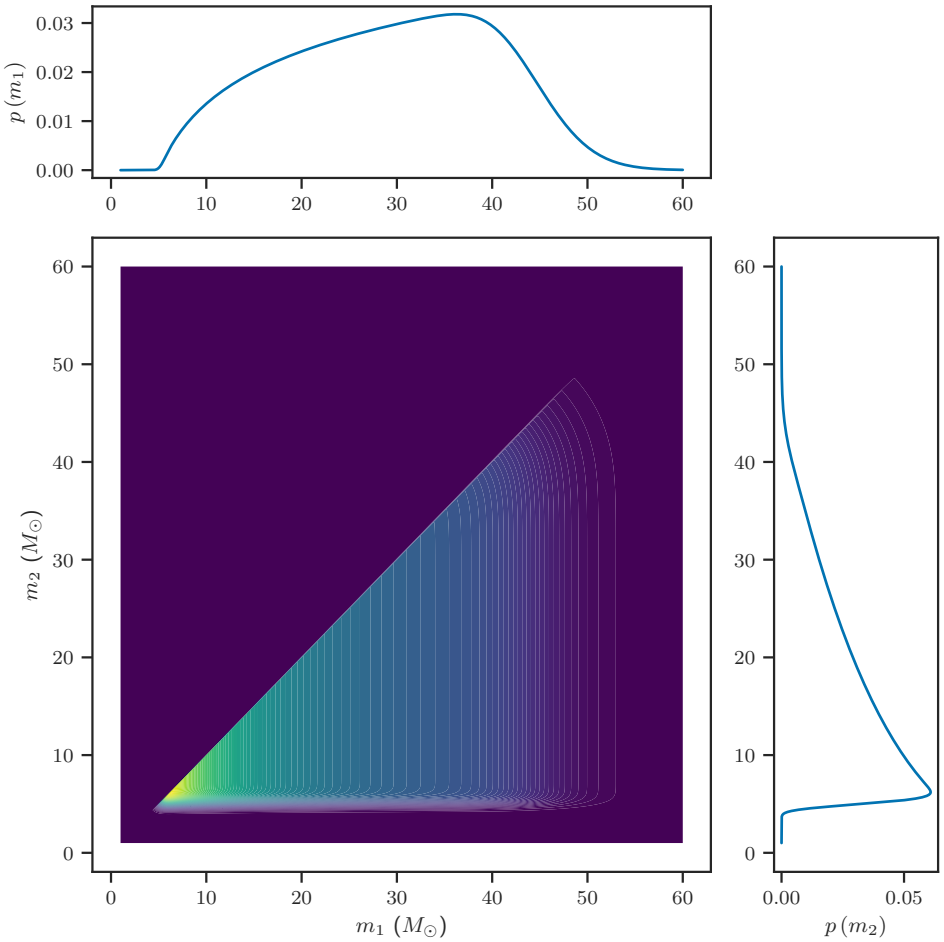

Extended Data Figure 1. Mass distributions. The joint and marginal mass distributions for the masses in merging BBH systems implied by the merger rate density in Eq. (A1) and the parameter choices in Eq. (A3). The turnover at $m \simeq 45\,M_\odot$ due to the PISN mass scale is apparent in the primary mass distribution.